

# Controlling the Dynamics of Atomic Correlations via the Coupling to a Dissipative Cavity

Catalin-Mihai Halati<sup>1</sup>, Ameneh Sheikhan<sup>2</sup>, Giovanna Morigi<sup>3</sup>, and Corinna Kollath<sup>2</sup>

<sup>1</sup>*Department of Quantum Matter Physics, University of Geneva, Quai Ernest-Ansermet 24, 1211 Geneva, Switzerland*

<sup>2</sup>*Physikalisches Institut, University of Bonn, Nussallee 12, 53115 Bonn, Germany*

<sup>3</sup>*Theoretische Physik, Universität des Saarlandes, Campus E26, D-66123 Saarbrücken, Germany*

(Received 29 March 2024; revised 5 September 2024; accepted 27 January 2025; published 21 February 2025)

We analyze the relaxation dynamics in an open system, composed by a quantum gas of bosons in a lattice interacting via both contact and global interactions. We report the onset of periodic oscillations of the atomic coherences exhibiting hallmarks of synchronization after a quantum quench. The dynamical behavior exhibits the many-body collapse and revival of atomic coherences and emerges from the interplay of the quantum dissipative nature of the cavity field and the presence of a (approximate) strong symmetry in the dissipative system. We further show that the approximate symmetry can dynamically self-organize. We argue that the approximate symmetry can be tailored to obtain long-lived coherences. These insights provide a general recipe to engineer the dynamics of globally interacting systems.

DOI: 10.1103/PhysRevLett.134.073604

Open system and measurement control have attracted an enormous interest in the last decade for the engineering of many-body quantum systems [1–6]. Most proposals target the creation of interesting steady states, e.g., topological states of fermionic matter [7], nontrivial transport properties [8], quantum phases stemming from long-range spin interactions [9–13] or exhibiting dynamical synthetic gauge fields [14–19]. Much less attention has been devoted to the design of environments affecting the dynamical properties of a quantum system [20–24]. In this case, the dynamics of correlations needs to be carefully considered [21]. For example, even though the BCS superconducting state itself can be prepared using dissipative dynamics [25], nevertheless, the desired superconducting current-current correlations are not present as long as the dissipative coupling is applied [21].

In this Letter, we present a general recipe on how to use the intricate interplay of dissipation and symmetries to engineer intriguing metastable and dynamical phenomena in open quantum systems. We exemplify this by designing long-lived synchronized oscillations of interacting bosonic atoms coupled to an optical cavity. The realization of long-lived coherences relies on employing dissipative state engineering and protecting the dynamics via strong symmetries, being related to purely imaginary eigenvalues of the Liouvillian operator, i.e., rotating coherences [26]. The coupling between atoms and cavity selectively stabilizes the atomic correlations, which can exhibit synchronization [27,28]. In the considered example, we select a spatiotemporal pattern such that the coherences between sites at even distances exhibit long-lived oscillations, while the coherences at odd distances are strongly suppressed [see sketch, Fig. 1(a)]. We show that the quantum nature of the cavity field is essential in determining this dynamics and that the

self-organization of the approximate symmetry can lead to a similar behavior.

One important element for understanding and tailoring the dissipative dynamics is the spectrum of the Liouvillian governing the evolution of the density matrix. The dissipative processes determine the complex nature of the

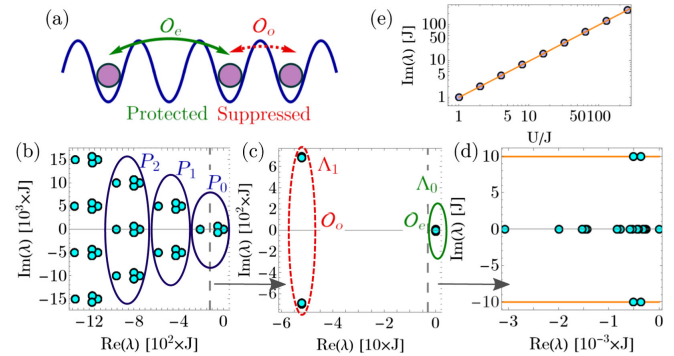


FIG. 1. (a) Sketch of ultracold atoms in an optical lattice potential. The operator  $\mathcal{O}_e$  probes the coherence between sites at even distance and  $\mathcal{O}_o$  at odd distance. (b)–(d) Eigenvalues spectra of the Liouvillian modeling the Bose-Hubbard model coupled to a dissipative cavity mode, Eq. (1), obtained with ED for  $L = 4$  sites,  $N = 2$  particles,  $\hbar\Omega\sqrt{N}/J = 1323$ ,  $\hbar\delta/J = 5000$ ,  $\hbar\Gamma/J = 750$ ,  $U/J = 10$ . We show the lowest (b) 1000 (c) 50 (d) 34 eigenvalues, where panels (c) and (d) are zoom ins of (b) and (c) at the right of the vertical dashed gray lines (as depicted by the gray arrows).  $P_n$  marks the subspaces containing  $n$  photonic excitations, with  $\Lambda_0$  and  $\Lambda_1$  corresponding to the decoherence free subspace and the first excited subspace for vanishing  $J$ .  $\mathcal{O}_e$  couples mainly to states in  $\Lambda_0$  and  $\mathcal{O}_o$  to states in  $\Lambda_1$ . (e) The dependence on the on-site interaction  $U$  of the imaginary part of the lowest eigenvalue whose imaginary part is in the range  $[0.75U, 1.25U]$ .

eigenvalues, which in the case of large dissipation rates  $\Gamma$ , are clustered in bands, with gaps between the real parts proportional to  $\Gamma$ . However, in many-body and hybrid systems, the situation can be much more complex and eigenstates can exist with decay rates smaller than  $\Gamma$ . For an atomic gas coupled to a lossy bosonic mode the Liouvillian  $\mathcal{L}$  is given by [29,30]

$$\frac{\partial}{\partial t}\rho = \mathcal{L}\rho = -\frac{i}{\hbar}[H, \rho] + \frac{\Gamma}{2}(2a\rho a^\dagger - a^\dagger a\rho - \rho a^\dagger a), \quad (1)$$

where  $a$  is the annihilation operator for the bosonic mode. An exemplary spectrum of  $\mathcal{L}$ , when  $H$  describes a Bose-Hubbard model coupled to a dissipative cavity, is shown in Fig. 1(b), determined using exact diagonalization (ED). Due to the direct dissipative coupling to the photon losses, most eigenstates of  $\mathcal{L}$  have eigenvalues whose real part is  $\propto \Gamma$ , e.g., in the subspaces  $P_1$  and  $P_2$ , signaling an exponential decay of their contribution to the time dependent density matrix. Instead, subspace  $P_0$  contains coherent photonic states that do not couple directly to dissipation and have a metastable nature, protected from the fast decay. Dissipative engineering [3] often employs the decoherence free subspace  $\Lambda_0$  (subspace of  $P_0$ ), i.e., corresponding to eigenvalues with vanishing real parts.

Generically, the Hamiltonian in Eq. (1) can be written as  $H = H_c + H_{ac} + H_a^{(1)} + H_a^{(2)}$ , where  $H_c$  describes the free bosonic mode,  $H_{ac} \propto (a + a^\dagger)\Delta$  contains the coupling of the mode to an atomic operator  $\Delta$ , and the other terms describing the atomic processes include  $H_a^{(1)}$ , which commutes with  $\Delta$ , and  $H_a^{(2)}$ , which does not commute with  $\Delta$ . In the limit of vanishing  $H_a^{(2)}$ , exciting possibilities arise to engineer dynamical features within the metastable subspace  $P_0$ , as in its absence a strong symmetry is present [26,31]. The symmetry generator  $\Delta$  commutes with both the Hamiltonian and the jump operator. This gives another handle on controlling the dynamics, as the evolution in distinct symmetry sectors is independent, each with its own steady or rotating states. Within  $P_0$ , the subspace  $\Lambda_1$  is generated by coherences between eigenstates of  $\Delta$  at different eigenvalues [32], while  $\Lambda_0$  contains steady states and coherences between degenerate eigenstates of  $\Delta$ . Furthermore,  $H_a^{(1)}$  can lift the degeneracy within the eigenspaces of  $\Delta$ . As a result, the Liouvillian can exhibit purely imaginary eigenvalues [32,45], offering a route for realizing synchronization. Thus, by designing the dissipative coupling, here via  $H_{ac}$ , we can choose which dynamical features are rapidly suppressed [e.g., in Fig. 1(c) correlations probing the excited subspace  $\Lambda_1$ ] and which are protected up to long times (with dynamics dominated by the lowest subspace  $\Lambda_0$ ). For example, the expectation value of an operator  $\mathcal{O}_o$  coupling only distinct eigenstates of  $\Delta$  [subspace  $\Lambda_1$  in Fig. 1(c)] experiences fast oscillations and rapid decay to its steady value, compared to  $\mathcal{O}_e$ , which

only couples degenerate eigenstates of  $\Delta$  [subspace  $\Lambda_0$  in Figs. 1(c) and 1(d)].

In the presence of the strong symmetry to probe the dynamics of the different symmetry sector one needs to carefully prepare the initial state. To circumvent this problem, we consider a finite contribution from  $H_a^{(2)}$ , which breaks the symmetry. If one slightly breaks a strong symmetry [46], it generally reduces the number of steady states, giving rise to slowly decaying states forming the subspace  $\Lambda_0$  within  $P_0$ . The decay timescale of these symmetry protected metastable states depends on the magnitude of the symmetry breaking term and can potentially be much smaller than the dissipative gaps of the Liouvillian in the presence of the strong symmetry. For example, the states shown in Fig. 1(e) would have zero real part in the limit  $H_a^{(2)} = 0$ ; however, even with a finite contribution their real parts are still much smaller than the gap to  $\Lambda_1$ . We envision these approximate strong symmetries as a tool for the design of metastable states of the Liouvillian [22,47–49], where we can control their lifetime by the magnitude of the symmetry breaking term. Thus, we consider a protocol in which we start from the ground state of  $H_a^{(1)} + H_a^{(2)}$ , containing the coherences of interest, and quench the coupling to the bosonic mode, considering a separation of scales with respect to the atomic processes. This induces the dissipative dynamics in the presence of the approximate strong symmetry.

We exemplify the recipe for a one-dimensional lattice of interacting bosonic atoms inside a high finesse cavity, transversely pumped with a standing-wave laser beam and exhibiting photon losses [50–52]. This showcases a dissipative many-body realization of the collapse and revival of coherences. Such dynamics has been discussed in closed systems for both matter and light fields [53–56], and has been observed for the matter field of a Bose-Einstein condensate [57], or nuclear spins [58]. For our example, the Hamiltonian contains  $H_c = \hbar\delta a^\dagger a$ , with  $\delta$  the cavity-pump detuning. The period of the lattice is chosen to be twice the period of the cavity mode, such that the cavity effectively couples to the even-odd atomic density imbalance,  $H_{ac} = -\hbar\Omega(a + a^\dagger)\Delta$ ,  $\Delta = \sum_j (-1)^j n_j$ , with the coupling strength  $\Omega$ . The coupling commutes with the atomic repulsive on-site interactions,  $H_a^{(1)} \equiv H_{\text{int}} = (U/2) \sum_{j=1}^{L-1} n_j(n_j - 1)$ , of strength  $U$ , and competes with the kinetic processes,  $H_a^{(2)} \equiv H_{\text{kin}} = -J \sum_{j=1}^{L-1} (b_j^\dagger b_{j+1} + \text{H.c.})$ , with amplitude  $J$ . Interacting bosonic lattice models coupled to an optical cavity have been realized experimentally [59–61], while theoretical studies focused mostly on steady state properties [46,51,52,62–74].

We analyze the quench scenario with the atoms in their ground state and the atoms-cavity coupling suddenly turned on. We perform the exact time evolution of Eq. (1) using a recently developed method based on time-dependent

matrix product states (tMPS); see Refs. [32,75]. We complement our understanding with analytical results in the limit  $J \rightarrow 0$  [32,75] and ED for small systems. These approaches go beyond the often employed mean-field treatment of the cavity-atoms coupling [52]. To emphasize the role of the cavity field, we contrast our tMPS results of the atom-cavity system with the dynamics of a Bose-Hubbard model in the presence of a classical light field, i.e., a superlattice potential. The superlattice potential  $V(t)$  can be obtained as a mean-field description of the coupled dynamics, Eq. (1), when the cavity is assumed to be a coherent state. The Hamiltonian in this situation is given by  $H_{\text{MF}} = H_{\text{int}} + H_{\text{kin}} - V(t)\Delta$  [32], and we refer to it as the classical field approach.

*Results in the presence of the approximate strong symmetry*—Our analysis begins in the regime of vanishing tunneling  $J = 0$ , where analytical results can be obtained [32]. This is motivated by the strong symmetry arising at  $J = 0$ , as local densities are conserved quantities, commuting with both  $H$  and  $a$  [26,31]. These results provide crucial information to our understanding also at small finite  $J$ , where the sectors of the symmetry are a good approximate description. We show the ED spectra of  $\mathcal{L}$  in Figs. 1(b)–1(d) for a small system, for parameters similar to the experiment performed in [60].

The subspaces  $P_n$ , in Fig. 1(b), correspond to excitations on top of the photonic coherent state, for which the main contribution to the real part is given by  $n\hbar\Gamma/2$  and by  $\hbar\delta$  to the imaginary part. The subspaces with  $n > 0$  show a fast decay and are important only for the short time dynamics. Therefore, we focus the analysis on  $P_0$ , and in particular on the lowest two subspaces  $\Lambda_1$  and  $\Lambda_0$ , Fig. 1(c). Here the photons are in a coherent state determined by the atomic density distribution.  $\Lambda_1$  contains excited states capturing the coherence between different atomic distribution characterized by imbalances  $\Delta$  and  $\Delta \pm 2$ . These coherences decay with a rate depending, at large dissipation strength, inversely on  $\Gamma$  [32], as known from the Zeno effect. In contrast,  $\Lambda_0$  consists of eigenstates with vanishing real part, protected by the strong symmetry for  $J = 0$ . As detailed in [32], there are several types of states in  $\Lambda_0$ , steady states of the form  $\rho_{0,st} = |\alpha(\Delta); \{n_j\}\rangle \langle \alpha(\Delta); \{n_j\}|$ , or traceless coherences  $\rho_0 = |\alpha(\Delta); \{n_j\}\rangle \langle \alpha(\Delta); \{n'_j\}|$  between states with different density distribution and the same odd-even imbalance. When the latter describes a coherence between states with different interaction energies, its eigenvalue has a finite imaginary part [orange line in Fig. 1(d)]. Such states are called rotating coherences and lead to persistent synchronized oscillations in the long-time limit [26–28]. We checked the dependence of the imaginary part on  $U$  for the ED results for small  $J$  in Fig. 1(e), recovering the linear dependence expected for  $J = 0$ .

We observe that a finite  $J$ , smaller than the  $J = 0$  gap between  $\Lambda_1$  and  $\Lambda_0$ , induces a finite real part to all eigenvalues, except one, lying in  $\Lambda_0$ , in Fig. 1(d). This

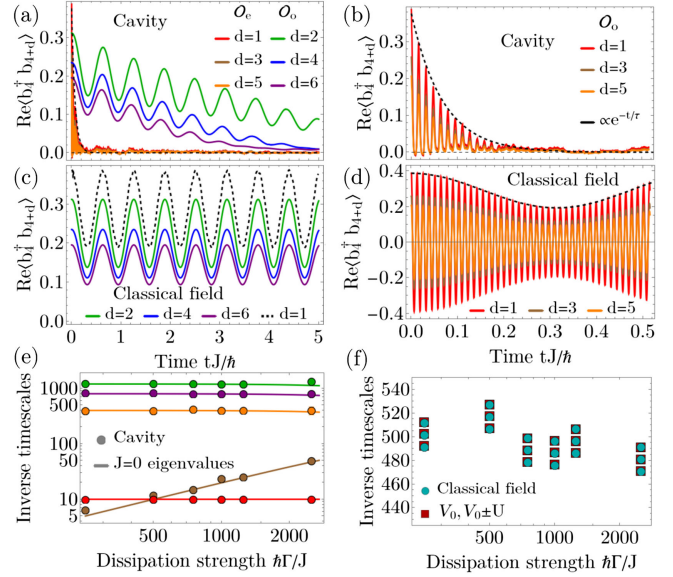


FIG. 2. Time evolution of the single particle correlations  $\text{Re}\langle b_4^\dagger b_{4+d} \rangle$ . (a),(b) The exact description of the cavity, Eq. (1), and (c),(d) classical field approach, for  $\hbar\Omega\sqrt{N}/J = 1323$ ,  $\hbar\delta/J = 5000$ ,  $\hbar\Gamma/J = 750$ ,  $U/J = 10$ ,  $N = 7$ ,  $L = 14$ . The dashed black curve in (a),(b) represents an exponential fit of the decay of the maxima for  $\text{Re}\langle b_4^\dagger b_5 \rangle$ . The dashed black curve in (c),(d) represents the interpolated behavior of the maxima of  $\text{Re}\langle b_4^\dagger b_5 \rangle$  for the classical field case. (e) Inverse timescales for dissipative quantum dynamics, the data is extracted from the tMPS evolution and the lines are the  $J = 0$  eigenvalues [32], with red  $|\text{Im}\lambda_0| = U$ , brown  $|\text{Re}\lambda_1| = [(2\hbar\Omega^2\Gamma)/(\delta^2 + \Gamma^2/4)]$ , and  $|\text{Im}\lambda_1| = [(4\hbar\Omega^2\delta)/(\delta^2 + \Gamma^2/4)](1 - \Delta)$  in green ( $\Delta = 7$ ), purple ( $\Delta = 5$ ) and orange ( $\Delta = 3$ ). (f) Inverse timescales for classical field dynamics, extracted from the numerical simulations with circles and the late time value of the potential  $V_0 = V(t \approx 5)$  and  $V_0 \pm U$  with squares.

marks the transition from multiple steady states due the strong symmetry to a single steady state in absence of the symmetry. The slight breaking of the symmetry creates a subspace of long-lived metastable states only weakly coupled to dissipation, which dominate the long-time dynamics, as seen in the time-evolution of the atomic correlations, Figs. 2(a) and 2(b) [same parameters as Figs. 1(b)–1(e)]. We depict the time-evolution of the single particle correlations,  $\text{Re}\langle b_4^\dagger b_{4+d} \rangle$ , obtained with the tMPS approach of simulating Eq. (1), for a larger system [32]. For odd distances  $d$  the correlations probe the evolution of the states contained in  $\Lambda_1$ , while for even distances  $d$  they probe the states in the subspace  $\Lambda_0$ . We observe extremely different timescales for odd and even correlations, reproducing very well the dynamics we aimed to engineer and characterized in terms of the approximate strong symmetry. At even distances the single particle correlations show oscillations [Fig. 2(a)], whose frequencies are determined by the value of  $U$  [red points and line in Fig. 2(e)]. The oscillations are only weakly damped on the tunneling

timescale  $J$ . In contrast, for odd distances both the frequencies of the oscillations and their exponential decay to a small value occur on much faster timescales [Figs. 2(a) and 2(b)]. We extract these timescales and obtain very good agreement with the analytical eigenvalues of  $\Lambda_1$  in Fig. 2(e) (brown for the decay rate and green, purple and orange for the frequencies). We note that at  $J = 0$  the synchronized oscillations are related to the fact that the operators  $b_i^\dagger b_{i+d}$ , for  $d$  even, can be used to construct the eigenstates with purely imaginary eigenvalues [27,28,32]. Similar dynamical behavior can also be observed in evolution of the pair correlations [32].

We highlight the importance of the dissipative quantum nature of the cavity by comparing with the case of a classical field realizing a superlattice potential  $H_{\text{MF}}$  [Figs. 2(a) and 2(b) in contrast to Figs. 2(c) and 2(d)]. For the single particle correlations at even distances the oscillation frequency is the same for the quantum and classical cases, given by  $U$ , but for the classical potential the oscillations do not show an attenuation for the times shown [Fig. 2(c)]. For odd distances the difference in behavior is even more striking, for the classical field the frequencies of the oscillations are given by the height of the potential and on-site interactions [see Figs. 2(d) and 2(e)], and the oscillations do not decay up to long times [dashed black line in Fig. 2(c)]. Thus, the suppression of the correlations at odd distances is due to the open quantum nature of the cavity and cannot be explained at a mean-field level by a classical superlattice potential. We note that the dynamical behavior cannot be recovered even if one adds stochastic noise in the dynamics of the classical coherent field [32].

*Photon number dynamics*—An interesting question is which timescales are reflected in the relaxation of the photon number. We observe in Fig. 3(a) that after an initial fast increase the photon number exhibits damped oscillations followed by a plateau. The oscillations frequency is

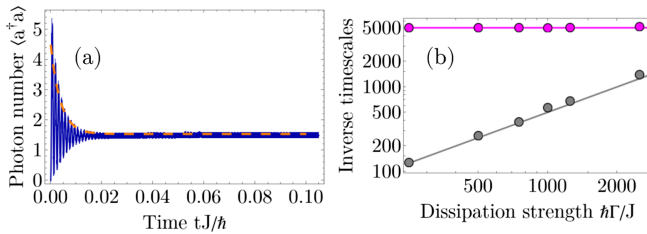


FIG. 3. (a) Time evolution of the photon number, Eq. (1). Dashed orange line corresponds to an exponential fit of the decay of the short time oscillations, with a decay rate  $\tau^{-1}/J = 261 \pm 12 \approx \hbar\Gamma/2J$ . (b) The frequency (magenta) and decay rate (gray) of the short time oscillations of the photon number versus  $\hbar\Gamma/J$ , the points correspond to the tMPS simulations and the lines are given by  $|\text{Re}\lambda_{p_1}| = \hbar\Gamma/2$  and  $|\text{Im}\lambda_{p_1}| = \hbar\delta$ . Parameters used are  $L = 14$ ,  $N = 7$ ,  $\hbar\delta/J = 5000$ ,  $U/J = 10$ , (a)  $\hbar\Omega\sqrt{N}/J = 6614$ ,  $\hbar\Gamma/J = 500$ , (b)  $\hbar\Omega\sqrt{N}/J = 1323$ .

consistent with the value of  $\delta$  and the fast decay with the inverse timescale of  $\Gamma/2$  [see Fig. 3(b) and [32]], corresponding to  $P_1$  [Fig. 1(b)]. We note that the photon number has not reached the steady state for the latest time shown; in Fig. 3(a), the long time dynamics corresponds to timescales set by the subspace  $\Lambda_0$ . Additional information is obtained by investigating the single quantum trajectories sampled in our numerical method. The photon number indicates that the trajectories are projected quickly to subspaces spanned by states with the same imbalance  $\Delta$  [32]. These results can be interpreted in connection with the phenomenon of dissipative freezing for the case of an approximate strong symmetry [46,76,77].

*Cavity-induced self-organized synchronization*—So far we made the connection between the timescales observed in the single particle correlations and the eigenvalues of the Liouvillian for small  $J$  in the regime of large detuning and dissipation. Next, we show that even in regimes initially far from the strong symmetry, due to the self-organization of the cavity-atom system, an approximate symmetry arises, protecting synchronized long-lived coherences. To show this, we consider the very challenging regime where all parameters are comparable; see Fig. 4. In this situation, it is much harder to obtain analytical insights or track individual eigenvalues in the spectrum, however, the tMPS method allows for simulations up to long times.

At strong atoms-cavity coupling, deep in the self-organized phase [71,72], we observe very similar synchronized oscillations in the atomic correlations at even distances as before, surviving up to very long times [Fig. 4(a)]. In contrast, for a coupling close to the self-organization threshold the oscillations are absent [Fig. 4(b)]. In order to

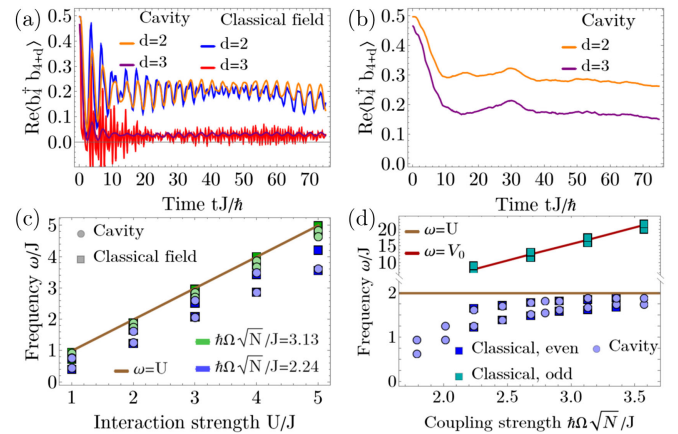


FIG. 4. (a),(b) Time evolution of the single particle correlations  $\text{Re}\langle b_4^\dagger b_{4+d} \rangle$  (a) for a strong coupling  $\hbar\Omega\sqrt{N}/J = 3.35$ , (b) for weak  $\hbar\Omega\sqrt{N}/J = 1.72$  and  $U/J = 2$ ,  $L = 14$ ,  $N = 7$ ,  $\hbar\Gamma/J = 1$ ,  $\hbar\delta/J = 2$ . (c),(d) Frequencies extracted from the dynamics of correlations as a function of  $U$  and  $\Omega$ . The lines at  $\omega = U$  (brown) and  $\omega = V_0$  (dark red) represent the expectation for the collapse and revival dynamics for a deep superlattice, where  $V_0 = V(t \approx 75)$ .

verify that the oscillations occurring in this regime are induced by coherences between states with different interaction energies, we compute the scaling of their frequency with  $U$  [Fig. 4(b)]. We obtain the linear scaling with  $U$  as for the ED results in Fig. 1(e) in the regime of small  $J$ . Furthermore, going deeper into the self-organized phase by increasing  $\hbar\Omega\sqrt{N}/J$ , the higher value of the two frequencies approaches the value  $U$ ; see Fig. 4(d). This implies that the states with coherences between configurations with the same imbalance, but different interaction energies, are long lived metastable states, producing the oscillations observed. For large  $\Omega$  the atoms feel a strong self-organized potential, suppressing the atomic tunneling and giving rise to an emergent approximate strong symmetry, similarly to small  $J$  regime. In contrast to the small  $J$  case, in this situation a similar synchronized oscillatory behavior and dependence of the frequencies is recovered from the simulations in a classical potential [Figs. 4(a)–4(d)] and the correlations at odd distances are not suppressed to such a small value as before, Fig. 4(a). After an initial decay the correlations saturate to a finite value comparable to the value obtained in the classical potential. However, in the classical potential the correlations at odd distances exhibit oscillations induced by the height of the potential [Fig. 4(d) upper part], not present for the coupling to the cavity.

**Conclusions**—We investigated how the dynamical properties of interacting atoms can be controlled by the coupling to the quantum field of a dissipative cavity. We show that by engineering the coupling to the cavity the dynamics of atomic correlations strongly depends on the distance between the sites they probe. In particular, for the single particle correlations at even distances we recover a dissipative analog of the collapse and revival behavior, exhibiting metastable synchronization, i.e., oscillatory evolution up to long times, with the frequency set by the atomic interactions. In contrast, the coherences at odd distances are strongly suppressed on short times, with the timescales set by the cavity parameters and atoms-cavity coupling strength. Important insights are obtained by considering the approximate strong symmetries of the open atoms-cavity system. The suppression of the odd correlations stems from the fact that they probe subspaces of the Liouvillian with large decay rates, while the dynamics of even correlations is contained close to the decoherence free subspace protected by the symmetry. This offers the opportunity to induce nontrivial dynamical behavior in other many-body dissipative quantum systems. We further show that the approximate symmetry can arise dynamically in self-organized regime. Experimentally, the synchronization dynamics of the coherences would be visible in the momentum distribution [32] obtained in time-of-flight measurements [57]. However, the momentum occupations have contributions from all single particle correlations, thus, to probe their very different evolution *in situ* coherence measurements would be needed.

**Acknowledgments**—We thank J. P. Brantut, T. Donner, T. Giamarchi, S. Jäger, H. Ritsch, L. Tolle, and C. Waechtler for fruitful discussions. We acknowledge support by the Swiss National Science Foundation under Division II Grant No. 200020-188687 and No. 200020-219400 and by the Deutsche Forschungsgemeinschaft (DFG, German Research Foundation) under Project No. 277625399-TRR 185 (B4), No. 277146847-CRC 1238 (C05), and under Germany’s Excellence Strategy—Cluster of Excellence Matter and Light for Quantum Computing (ML4Q) EXC 2004/1–390534769. This research was supported in part by the National Science Foundation under Grant No. NSF PHY-1748958 and No. PHY-2309135. G. M. acknowledges support from the Deutsche Forschungsgemeinschaft (DFG, German Research Foundation)—Project-ID 429529648-TRR 306 QuCoLiMa (“Quantum Cooperativity of Light and Matter”).

**Data availability**—The supporting data for this article are openly available at Zenodo [78].

- 
- [1] S. Diehl, A. Micheli, A. Kantian, B. Kraus, H. P. Büchler, and P. Zoller, Quantum states and phases in driven open quantum systems with cold atoms, *Nat. Phys.* **4**, 878 (2008).
  - [2] F. Verstraete, M. M. Wolf, and J. Ignacio Cirac, Quantum computation and quantum-state engineering driven by dissipation, *Nat. Phys.* **5**, 633 (2009).
  - [3] M. Müller, S. Diehl, G. Pupillo, and P. Zoller, Engineered open systems and quantum simulations with atoms and ions, *Adv. At. Mol. Opt. Phys.* **61**, 1 (2012).
  - [4] H. M. Wiseman and G. J. Milburn, *Quantum Measurement and Control* (Cambridge University Press, Cambridge, England, 2009), 10.1017/CBO9780511813948.
  - [5] J. Zhang, Y. xi Liu, R.-B. Wu, K. Jacobs, and F. Nori, Quantum feedback: Theory, experiments, and applications, *Phys. Rep.* **679**, 1 (2017).
  - [6] D. A. Puente, F. Motzoi, T. Calarco, G. Morigi, and M. Rizzi, Quantum state preparation via engineered ancilla resetting, *Quantum* **8**, 1299 (2024).
  - [7] C.-E. Bardyn, M. A. Baranov, C. V. Kraus, E. Rico, A. İmamoğlu, P. Zoller, and S. Diehl, Topology by dissipation, *New J. Phys.* **15**, 085001 (2013).
  - [8] G. T. Landi, D. Poletti, and G. Schaller, Nonequilibrium boundary-driven quantum systems: Models, methods, and properties, *Rev. Mod. Phys.* **94**, 045006 (2022).
  - [9] F. Mivehvar, H. Ritsch, and F. Piazza, Cavity-quantum-electrodynamical toolbox for quantum magnetism, *Phys. Rev. Lett.* **122**, 113603 (2019).
  - [10] S. Ostermann, H.-W. Lau, H. Ritsch, and F. Mivehvar, Cavity-induced emergent topological spin textures in a Bose–Einstein condensate, *New J. Phys.* **21**, 013029 (2019).
  - [11] N. Masalaeva, W. Niedenzu, F. Mivehvar, and H. Ritsch, Spin and density self-ordering in dynamic polarization gradients fields, *Phys. Rev. Res.* **3**, 013173 (2021).
  - [12] A. Chiochetta, D. Kiese, C. P. Zelle, F. Piazza, and S. Diehl, Cavity-induced quantum spin liquids, *Nat. Commun.* **12**, 5901 (2021).

- [13] P. Urich, S. Bandyopadhyay, N. Sauerwein, J. Sonner, J.-P. Brantut, and P. Hauke, A cavity quantum electrodynamics implementation of the Sachdev–Ye–Kitaev model, [arXiv: 2303.11343](https://arxiv.org/abs/2303.11343).
- [14] C. Kollath, A. Sheikhan, S. Wolff, and F. Brennecke, Ultracold fermions in a cavity-induced artificial magnetic field, *Phys. Rev. Lett.* **116**, 060401 (2016).
- [15] A. Sheikhan, F. Brennecke, and C. Kollath, Cavity-induced generation of nontrivial topological states in a two-dimensional Fermi gas, *Phys. Rev. A* **94**, 061603(R) (2016).
- [16] K. E. Ballantine, B. L. Lev, and J. Keeling, Meissner-like effect for a synthetic gauge field in multimode cavity QED, *Phys. Rev. Lett.* **118**, 045302 (2017).
- [17] C.-M. Halati, A. Sheikhan, and C. Kollath, Cavity-induced artificial gauge field in a Bose-Hubbard ladder, *Phys. Rev. A* **96**, 063621 (2017).
- [18] F. Mivehvar, H. Ritsch, and F. Piazza, Superradiant topological peierls insulator inside an optical cavity, *Phys. Rev. Lett.* **118**, 073602 (2017).
- [19] E. Colella, F. Mivehvar, F. Piazza, and H. Ritsch, Hofstadter butterfly in a cavity-induced dynamic synthetic magnetic field, *Phys. Rev. B* **100**, 224306 (2019).
- [20] D. Poletti, P. Barmettler, A. Georges, and C. Kollath, Emergence of glasslike dynamics for dissipative and strongly interacting bosons, *Phys. Rev. Lett.* **111**, 195301 (2013).
- [21] B. Sciolla, D. Poletti, and C. Kollath, Two-time correlations probing the dynamics of dissipative many-body quantum systems: Aging and fast relaxation, *Phys. Rev. Lett.* **114**, 170401 (2015).
- [22] K. Macieszczak, M. Guță, I. Lesanovsky, and J. P. Garrahan, Towards a theory of metastability in open quantum dynamics, *Phys. Rev. Lett.* **116**, 240404 (2016).
- [23] A. del Campo and K. Kim, Focus on shortcuts to adiabaticity, *New J. Phys.* **21**, 050201 (2019).
- [24] E. C. King, L. Giannelli, R. Menu, J. N. Kriel, and G. Morigi, Adiabatic quantum trajectories in engineered reservoirs, *Quantum* **8**, 1428 (2024).
- [25] W. Yi, S. Diehl, A. J. Daley, and P. Zoller, Driven-dissipative many-body pairing states for cold fermionic atoms in an optical lattice, *New J. Phys.* **14**, 055002 (2012).
- [26] V. V. Albert and L. Jiang, Symmetries and conserved quantities in Lindblad master equations, *Phys. Rev. A* **89**, 022118 (2014).
- [27] B. Buča, J. Tindall, and D. Jaksch, Non-stationary coherent quantum many-body dynamics through dissipation, *Nat. Commun.* **10**, 1730 (2019).
- [28] B. Buča, C. Booker, and D. Jaksch, Algebraic theory of quantum synchronization and limit cycles under dissipation, *SciPost Phys.* **12**, 097 (2022).
- [29] H. Carmichael, *An Open Systems Approach to Quantum Optics* (Springer Verlag, Berlin, Heidelberg, 1991), 10.1007/978-3-540-47620-7.
- [30] H. P. Breuer and F. Petruccione, *The Theory of Open Quantum Systems* (Oxford University Press, Oxford, 2002), 10.1093/acprof:oso/9780199213900.001.0001.
- [31] B. Buča and T. Prosen, A note on symmetry reductions of the Lindblad equation: Transport in constrained open spin chains, *New J. Phys.* **14**, 073007 (2012).
- [32] See Supplemental Material at <http://link.aps.org/supplemental/10.1103/PhysRevLett.134.073604> for details on the time-dependent matrix product states approach (tMPS), the model we consider in the case of a classical superlattice potential, the results for the case of a classical field under the action of a stochastic noise, the analytical derivations of the eigenvalues and eigenstates of the Liouvillian in the limit of vanishing hopping, the momentum distributions, the dynamics of single particle and pair correlations for an alternative initial state, and the dynamics of quantum trajectories. Supplemental Material includes Refs. [33–44].
- [33] C.-M. Halati, External control of many-body quantum systems, Ph.D. thesis, University of Bonn, 2021, <https://hdl.handle.net/20.500.11811/9343>.
- [34] J. Dalibard, Y. Castin, and K. Mølmer, Wave-function approach to dissipative processes in quantum optics, *Phys. Rev. Lett.* **68**, 580 (1992).
- [35] C. W. Gardiner, A. S. Parkins, and P. Zoller, Wave-function quantum stochastic differential equations and quantum-jump simulation methods, *Phys. Rev. A* **46**, 4363 (1992).
- [36] A. J. Daley, Quantum trajectories and open many-body quantum systems, *Adv. Phys.* **63**, 77 (2014).
- [37] S. R. White and A. E. Feiguin, Real-time evolution using the density matrix renormalization group, *Phys. Rev. Lett.* **93**, 076401 (2004).
- [38] A. J. Daley, C. Kollath, U. Schollwöck, and G. Vidal, Time-dependent density-matrix renormalization-group using adaptive effective Hilbert spaces, *J. Stat. Mech.* (2004) P04005.
- [39] U. Schollwöck, The density-matrix renormalization group in the age of matrix product states, *Ann. Phys. (Amsterdam)* **326**, 96 (2011).
- [40] E. M. Stoudenmire and S. R. White, Minimally entangled typical thermal state algorithms, *New J. Phys.* **12**, 055026 (2010).
- [41] M. L. Wall, A. Safavi-Naini, and A. M. Rey, Simulating generic spin-boson models with matrix product states, *Phys. Rev. A* **94**, 053637 (2016).
- [42] M. Fishman, S. R. White, and E. M. Stoudenmire, The ITENSOR software library for tensor network calculations, *SciPost Phys. Codebases* **4** (2022), 10.21468/SciPostPhysCodeb.4.
- [43] D. Nagy, G. Szirmai, and P. Domokos, Self-organization of a Bose-Einstein condensate in an optical cavity, *Eur. Phys. J. D* **48**, 127 (2008).
- [44] S. Schütz, H. Habibian, and G. Morigi, Cooling of atomic ensembles in optical cavities: Semiclassical limit, *Phys. Rev. A* **88**, 033427 (2013).
- [45] V. V. Albert, Asymptotics of quantum channels: Conserved quantities, an adiabatic limit, and matrix product states, *Quantum* **3**, 151 (2019).
- [46] C.-M. Halati, A. Sheikhan, and C. Kollath, Breaking strong symmetries in dissipative quantum systems: Bosonic atoms coupled to a cavity, *Phys. Rev. Res.* **4**, L012015 (2022).
- [47] J. J. García-Ripoll, S. Dürr, N. Syassen, D. M. Bauer, M. Lettner, G. Rempe, and J. I. Cirac, Dissipation-induced hard-core boson gas in an optical lattice, *New J. Phys.* **11**, 013053 (2009).
- [48] P. Zanardi and L. Campos Venuti, Coherent quantum dynamics in steady-state manifolds of strongly dissipative systems, *Phys. Rev. Lett.* **113**, 240406 (2014).

- [49] Y.-D. Jin, C.-D. Qiu, and W.-L. Ma, Theory of metastability in discrete-time open quantum dynamics, *Phys. Rev. A* **109**, 042204 (2024).
- [50] C. Maschler, I. B. Mekhov, and H. Ritsch, Ultracold atoms in optical lattices generated by quantized light fields, *Eur. Phys. J. D* **46**, 545 (2008).
- [51] H. Ritsch, P. Domokos, F. Brennecke, and T. Esslinger, Cold atoms in cavity-generated dynamical optical potentials, *Rev. Mod. Phys.* **85**, 553 (2013).
- [52] F. Mivehvar, F. Piazza, T. Donner, and H. Ritsch, Cavity QED with quantum gases: New paradigms in many-body physics, *Adv. Phys.* **70**, 1 (2021).
- [53] F. W. Cummings, Stimulated emission of radiation in a single mode, *Phys. Rev.* **140**, A1051 (1965).
- [54] J. H. Eberly, N. B. Narozhny, and J. J. Sanchez-Mondragon, Periodic spontaneous collapse and revival in a simple quantum model, *Phys. Rev. Lett.* **44**, 1323 (1980).
- [55] E. M. Wright, D. F. Walls, and J. C. Garrison, Collapses and revivals of Bose-Einstein condensates formed in small atomic samples, *Phys. Rev. Lett.* **77**, 2158 (1996).
- [56] S. Dooley, F. McCrossan, D. Harland, M. J. Everitt, and T. P. Spiller, Collapse and revival and cat states with an  $N$ -spin system, *Phys. Rev. A* **87**, 052323 (2013).
- [57] M. Greiner, O. Mandel, T. W. Hänsch, and I. Bloch, Collapse and revival of the matter wave field of a Bose-Einstein condensate, *Nature (London)* **419**, 51 (2002).
- [58] R. M. Goldblatt, A. M. Martin, and A. A. Wood, Sensing coherent nuclear spin dynamics with an ensemble of paramagnetic nitrogen spins, *PRX Quantum* **5**, 020334 (2024).
- [59] J. Klinder, H. Keßler, M. R. Bakhtiari, M. Thorwart, and A. Hemmerich, Observation of a superradiant Mott insulator in the Dicke-Hubbard model, *Phys. Rev. Lett.* **115**, 230403 (2015).
- [60] R. Landig, L. Hruby, N. Dogra, M. Landini, R. Mottl, T. Donner, and T. Esslinger, Quantum phases from competing short- and long-range interactions in an optical lattice, *Nature (London)* **532**, 476 (2016).
- [61] L. Hruby, N. Dogra, M. Landini, T. Donner, and T. Esslinger, Metastability and avalanche dynamics in strongly correlated gases with long-range interactions, *Proc. Natl. Acad. Sci. U.S.A.* **115**, 3279 (2018).
- [62] W. Niedenzu, R. Schulze, A. Vukics, and H. Ritsch, Microscopic dynamics of ultracold particles in a ring-cavity optical lattice, *Phys. Rev. A* **82**, 043605 (2010).
- [63] A. O. Silver, M. Hohenadler, M. J. Bhaseen, and B. D. Simons, Bose-Hubbard models coupled to cavity light fields, *Phys. Rev. A* **81**, 023617 (2010).
- [64] S. Fernández-Vidal, G. De Chiara, J. Larson, and G. Morigi, Quantum ground state of self-organized atomic crystals in optical resonators, *Phys. Rev. A* **81**, 043407 (2010).
- [65] Y. Li, L. He, and W. Hofstetter, Lattice-supersolid phase of strongly correlated bosons in an optical cavity, *Phys. Rev. A* **87**, 051604(R) (2013).
- [66] M. R. Bakhtiari, A. Hemmerich, H. Ritsch, and M. Thorwart, Nonequilibrium phase transition of interacting bosons in an intra-cavity optical lattice, *Phys. Rev. Lett.* **114**, 123601 (2015).
- [67] T. Flottat, L. d. F. de Parny, F. Hébert, V. G. Rousseau, and G. G. Batrouni, Phase diagram of bosons in a two-dimensional optical lattice with infinite-range cavity-mediated interactions, *Phys. Rev. B* **95**, 144501 (2017).
- [68] E. I. Rodríguez Chiacchio and A. Nunnenkamp, Tuning the relaxation dynamics of ultracold atoms in a lattice with an optical cavity, *Phys. Rev. A* **97**, 033618 (2018).
- [69] R. Lin, L. Papariello, P. Mollignini, R. Chitra, and A. U. J. Lode, Superfluid-Mott-insulator transition of ultracold superradiant bosons in a cavity, *Phys. Rev. A* **100**, 013611 (2019).
- [70] L. Himbert, C. Cormick, R. Kraus, S. Sharma, and G. Morigi, Mean-field phase diagram of the extended Bose-Hubbard model of many-body cavity quantum electrodynamics, *Phys. Rev. A* **99**, 043633 (2019).
- [71] C.-M. Halati, A. Sheikhan, H. Ritsch, and C. Kollath, Numerically exact treatment of many-body self-organization in a cavity, *Phys. Rev. Lett.* **125**, 093604 (2020).
- [72] A. V. Bezvershenko, C.-M. Halati, A. Sheikhan, C. Kollath, and A. Rosch, Dicke transition in open many-body systems determined by fluctuation effects, *Phys. Rev. Lett.* **127**, 173606 (2021).
- [73] S. Sharma, S. B. Jäger, R. Kraus, T. Roscilde, and G. Morigi, Quantum critical behavior of entanglement in lattice bosons with cavity-mediated long-range interactions, *Phys. Rev. Lett.* **129**, 143001 (2022).
- [74] T. Chanda, R. Kraus, J. Zakrzewski, and G. Morigi, Bond order via cavity-mediated interactions, *Phys. Rev. B* **106**, 075137 (2022).
- [75] C.-M. Halati, A. Sheikhan, and C. Kollath, Theoretical methods to treat a single dissipative bosonic mode coupled globally to an interacting many-body system, *Phys. Rev. Res.* **2**, 043255 (2020).
- [76] C. Sánchez Muñoz, B. Buča, J. Tindall, A. González-Tudela, D. Jaksch, and D. Porras, Symmetries and conservation laws in quantum trajectories: Dissipative freezing, *Phys. Rev. A* **100**, 042113 (2019).
- [77] J. Tindall, D. Jaksch, and C. S. Muñoz, On the generality of symmetry breaking and dissipative freezing in quantum trajectories, *SciPost Phys. Core* **6**, 004 (2023).
- [78] C.-M. Halati, A. Sheikhan, G. Morigi, and C. Kollath, Figure data for article “Controlling the dynamics of atomic correlations via the coupling to a dissipative cavity” [Data set], Zenodo, [10.5281/zenodo.10890066](https://doi.org/10.5281/zenodo.10890066) (2024).